Influence of heat tightness of an enclosure fire on ignition risk of unburnt gases in a connected exhaust system – An experimental study

Brady Manescau, Hui-Ying Wang, Bruno Coudour, Jean-Pierre Garo

Influence of Heat Tightness of an Enclosure Fire on Ignition Risk of Unburnt Gases in a Connected Exhaust System – An Experimental Study

Brady MANESCAU, Hui-Ying WANG, Bruno COUDOUR and Jean Pierre GARO

Institut Pprime : Fluides-Thermique-Combustion, CNRS, ENSMA, Université de Poitiers
BP 40109
F86961 Futuroscope Chasseneuil Cedex, France

wang@ensma.fr

ABSTRACT

An experimental study was performed from a reduced scale enclosure with a length/height and width of 2 m. A dodecane pan of 40 cm in diameter is placed at the center of the enclosure floor. An external ventilation system provides an air supply rate with an Air Change Per Hour (ACPH) ranging from 3 to 5. Influence of the intermediate levels of thermal insulation of enclosure on ignition risk in a connected exhaust system is experimentally evaluated. The results show that thermal insulation of an enclosure leads to faster fire growth, implying more important peak in heat release rate, and thus more dangerous fire in regards to the ignition risk. Heat tightness of enclosure enhances the mass loss rate of liquid fuel, but reduces the air supply rate from the admission duct due to decrease of the depression level in the compartment. As a consequence, the fire becomes quickly very-under-ventilated, and a large vaporized fuel is converted into the unburnt gases such as hydrocarbons, CO and H_2. In the early stages of a fire, a hotter unburnt fuel layer with a concentration above the Lower Flammability Limit (LFL) is formed in the extraction duct connected to a mechanically ventilated enclosure fire. With a long time delay in a range of 16 to 21 min in the current study, the energy released per mass of oxygen consumed allows to raise the smoke temperature above 350°C. Occurrence of flame extinction in vitiated air enclosure makes a sudden increase of the depression level inside enclosure due to cooling effects. This results in a sudden supply of fresh air from dilution duct, providing a sufficient amount of oxygen to trigger ignition of a fuel rich mixture near the extraction duct. It is found that ignition of unburnt volatiles at entrance of the extraction duct occurs more easily when the compartment is more heat-tight with a reduction by about 30% in the ignition delay.

KEYWORDS:
fire growth; ignition risk; compartment fire; liquid fuel; heat tightness; extraction duct; dilution duct; depression

INTRODUCTION

Explosions or gas deflagrations caused by re-ignition have gained increasing attention typically when a compartment containing a fire has a very limited fresh air supply during its extinction phase. Intensive research has been focused on the phenomenological analysis of backdraught in an enclosure after flame exhaust if there is a sudden supply of fresh air, e.g. due to a window or door opening or breaking, possibly due to the fire [1, 2]. The experimental study of Lassus et al. [3] showed that even in a highly confined setting, an extraction duct is an important pathway for the onset of re-ignition of a fuel rich mixture if there is a sudden supply of fresh air from an interconnecting ventilation system. Fundamental research [4-8] has been also carried on the phenomena of periodic oscillations and temporary flame quenching in a highly

confined compartment equipped with mechanically ventilation system. The oscillation is caused by phenomenon of ghosting flame where the flame moves away from the pool and towards the air inlet [6]. The low-frequency oscillating flames with a drastic change in flame behavior were experimentally observed in a vitiated air enclosure [7, 8]. They postulated that issues involved for such oscillatory behavior are evaporation rate of condensed fuel [5], phenomena leading to a reverse flow in the supply ventilation system [4] and successive combustion of unburnt gases [5, 8].

As a condensed fuel, liquid pool fires usually generate a significant hazard in an enclosure due to large amount of unburnt volatile gases. The liquids could originate e.g. from leaks of transformers generators or other machinery. Knowing the liquid fire burning rate is the starting point of any fire safety analysis. Some empirical correlations [9, 10, 11] for mass loss rate of a liquid fuel is limited to the large enclosure where the heat fluxes from hot wall can be negligible. A global approach [12, 13, 14] for the mass burning flux of liquid fire is based on the measured radiative heat feedback to the condensed fuel surface or flame temperature. The burning rate of liquid pool can be significantly different in highly confined spaces, essentially attributed to the influence of air ventilation, heat radiation from hot walls and gas layer [15]. The existing empirical correlations [9-14] cannot take into account the factors such as oscillating flames and hot walls which affect significantly burning rate of the liquid pool fires in a highly confined enclosure. The quantitative agreement between experimental data and fully predictive simulation is again fair concerning the burning rate of liquid fuel in an enclosure [16]. Only using the mass loss rate collected experimentally, numerical simulation manages to correctly predict the thermal behaviour [17], visibility [18] and pressure [19] for the mechanically ventilated compartments.

In order to contain the potential release of radioactive material and avoid dispersion to the outside, nuclear installations are built with increasingly air/ heat-tight envelopes [4]. Thermal insulation of enclosure is as such particularly relevant not only for Nuclear Power Plants [4], but also probably for an increasingly popular low-energy consumption type of building [20]. Heat-tightness in buildings envelopes has high potential in energy demand reduction and consequently in energy savings [21]. Air or heat-tight envelopes can sufficiently increase the peak overpressure and temperature from fast-growing fires to cause structural damage [19]. The increased pressure and temperature were identified [19, 21] as one of the consequences of better energy efficiency, resulting in a reverse flow in the supply ventilation system [4]. The effect of heat permeability of enclosure has an importance on the fire behavior, notably on the thermal stratification of unburnt fuel gases [22]. The more heat-tight is a compartment, the more heat feedback is received to the surface of burning liquid fuel [23]. The re-ignition related risks may become more significant when the enclosure is more heat-tight due to a large formation of unburnt fuel. In this work, the investigation aims to identify experimentally the impact of thermal insulation of an enclosure on both the burning rate of liquid pool and ignition delay at entrance of the extraction duct.

EXPERIMENTAL SET-UP

The schematic experimental facility with a 2 m in length/height and width is shown in Figure 1(a, b, c). An external ventilation system consists of two intake ducts and an extraction duct. The intake was placed closer to the floor at a height of 0.3 m and the exhaust was placed near the ceiling at a height of 1.7 m. The extraction duct has a length of 1.1 m, and the dilution duct has a length of 2.5 m. Ducts have a square section of 0.2x0.2 m^2.

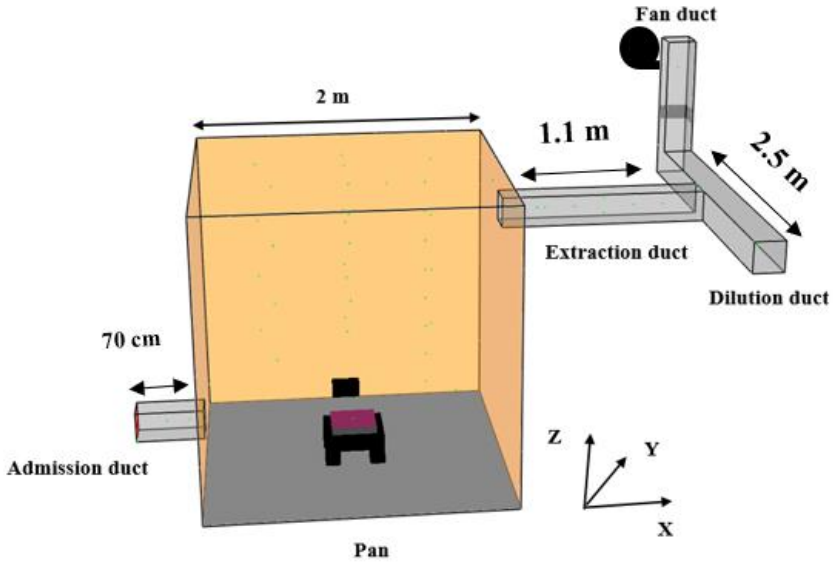

1a) 3D view of the experimental facility

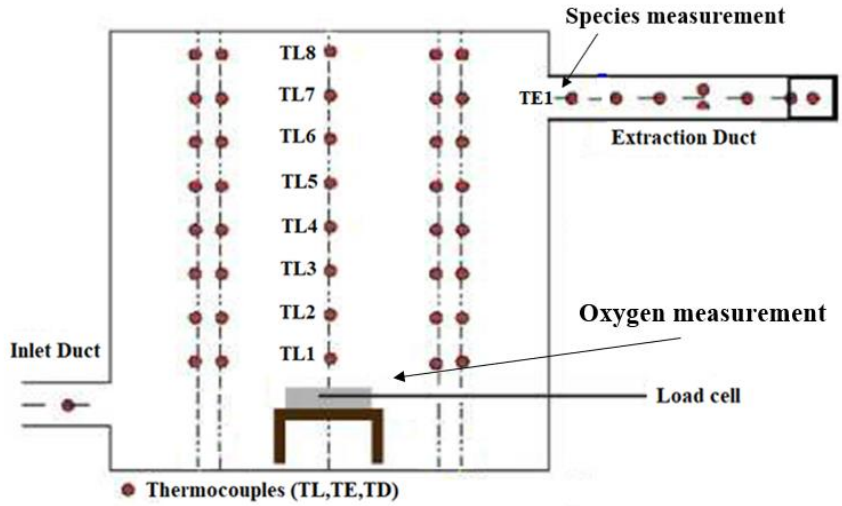

1b) side (x, z) view for the measurement locations

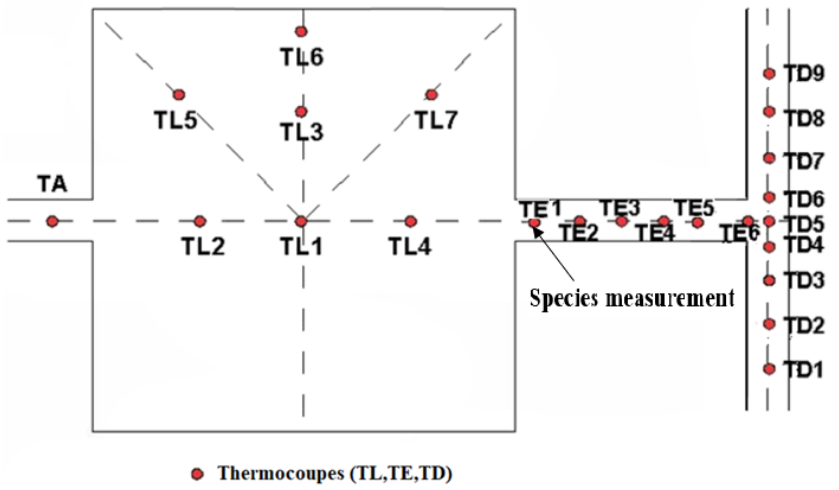

1c) measurement positions from the top (x, y) view

Figure 1. Mechanically ventilated enclosure fire connected to an extraction duct

Theoretically, the total flow loss in the duct from wall friction and duct fittings are assigned as dimensionless loss numbers to the ducts, as :

$$K = \frac{f\,L}{D} \qquad (1)$$

where D and L are the duct diameter and length, respectively. The parameter, f, can be estimated from an approximation [24]. In the current work, all ducts are made of smooth galvanized steel, and the ventilation ducts can be considered as non-rough. This allows to neglect the regular pressure losses, and consider only the singular head losses. The air flow rates at the intake and dilution ducts are regulated as a function of the depression level by means of an adjustment of rectangular flaps located upstream of these ducts, which can generate an aeraulic resistances. The pressure difference between the inside and outside is adjusted only in non-fire conditions. The experimental facility is not perfectly airtight mainly due to passage of the thermocouples through the wall and door gap. A leak of area in the order of 12-14 cm^2 [25] was estimated from conservation of the volume flow rate at the admission and extraction ducts as a function of the depression level.

A mechanical extraction is carried out by using System-Air Euro S7440, providing a maximum volume flow rate of 720 m^3/h, and pressure difference of $\Delta P_{max} = 186\,Pa$. This is a centrifugal fan with single-phase variable speed to select the desired airflow rate [25]. As shown in Fig.1a, the fan is placed at the outlet of a duct orthogonal to the dilution duct at a height of 2.6 m. The fan characteristic curve (i.e., delivered flow rate as a function of pressure) is shown in Fig.2. Before activating the fire, a period of 10 minute was included for establishing a depression below atmospheric pressure inside the enclosure. The depression level depends on the Air Change Per Hour (ACPH) of the enclosure with a range from 3 to 5, corresponding to a volume flow rate of 24 and 40 m^3/h, respectively. The air inlet velocity in non-fire conditions varies from 0.1667 m/s (3 ACPH) to 0.2778 m/s (5 ACPH). After activating the fire, velocity, temperature and pressure inside the enclosure as well as the ventilation ducts depend on the fire dynamic.

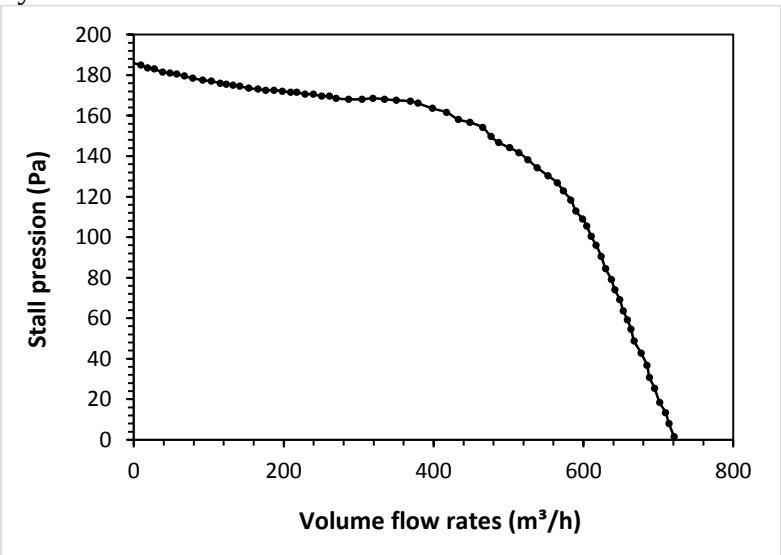

Figure 2. Relationship between the stall pressure and the free volume flow rate of the fan

In our previous work [25], a circular heptane or dodecane pan with a diameter varying from 23 to 40 cm was employed. A series of fire experiment were conducted by combining the three parameters such as pool size, ACPH and fuel type for investigating the extinction/ignition phenomena. In this work, a stainless-steel circular pan with a diameter of 40 cm was chosen. The liquid fuel pan was placed in the middle of the enclosure, slightly elevated at a height of 0.3 m. Dodecane is typically used as the fuel load, and occurrence of an auto-ignition was identified experimentally. The fuel mass was continuously monitored using a load cell, installed under the pan. The performed measurements include pressure, temperature and chemical species concentrations of gases filling the enclosure. A good repeatability was obtained with a difference below 5% regarding the temperature measurements and the mass loss rate during each fire tests. As shown in Fig.1b, c), the gas temperature was analyzed from different vertical profiles inside the enclosure, at the extraction duct and at the dilution one. Each of the vertical profiles comprises eight thermocouples positioned at regular intervals of 0.2 m over the height of the enclosure.

Two situations are taken into account for the intermediate levels of thermal insulation of enclosure. In the first situation, walls of the enclosure are made of 20-cm-thick cellular concrete with a thermal conductivity of λ =1 W/m/K, a density of ρ =860 kg/m^3, and a specific heat of C_p=0.88 kJ/kg/K. There is a relatively strong conductive heat loss via the walls during fire tests, and such case is named as 'heat loss'. In the second situation, the 20-cm-thick cellular concrete walls and ceiling are recovered by a 3.5-cm-thick insulating material as Promatech H with the following properties : λ = 0.175 W/m.K, ρ =400 kg/m^3 and C_p=0.92 kJ/kg.K. In such case, the conductive heat loss via the walls becomes rather weak, and the enclosure is considered as 'heat tightness' or 'thermal insulation'. The reduction in the volume with an insulating material is low than 8%, and affects somewhat the amount of oxygen initially present in the enclosure. But the different wall thicknesses do not affect the oxygen supply rate by mechanical ventilation, and thus, the occurrence of auto-ignition of unburnt gas near the extraction duct.

Since experiments in full scale are expensive, the numbers of tests are limited. With reduced-scale enclosure, more tests may be carried out but the scale reduction must respect several scaling laws adapted to the studied problem. Fire compartment tests have been conducted at a reduced geometric scale, maintaining a constant Froude number, $Fr=u^2/gL$ where L and u denote the characteristic length and velocity, respectively. Reynolds number is large enough to ensure the turbulence of the flow. The Froude number is then made constant by $u \propto L^{1/2}$ that comes from dimensionless variable of momentum conservation. Flow time scale is obtained from mass conservation by $\tau \propto \frac{L}{u} \propto L^{1/2}$. Since the ventilation flow rate is the inverse of τ, it scales with $L^{-1/2}$. From dimensionless variable of the energy equation, the source term contains the Zukoski number [26], defined as $\frac{\dot{Q}}{Fr\, L^{5/2}\, (\rho C_p T)\, g^{1/2}}$. In order to obtain a similitude between a full scale and a reduced scale compartments, a constant Froude number (Fr) must be maintained, and the ratio ($\dot{Q}^2/L^5$) between heat release rate ($\dot{Q}$) and characteristic length (L) should be preserved. Based on this concept, our reduced scale experimental device with a volume of 8 m^3 corresponds to a full scale 100 m^3 compartment with a HRR below 1 MW.

RESULTS AND DISCUSSION

Histories of the relative pressure (P_0-P) for 3 and 5 ACPH are illustrated in Figure 3(a, b). Here, P_0 denotes the atmospheric pressure, and P the enclosure one. The fire-induced pressure can be said to follow three main stages : 1) activating the fire causes an overpressure inside the compartment; 2) with some time delay, the fully developed fire becomes ventilation controlled due to lack of oxygen with appearance of pressure oscillations; 3) occurrence of flame extinction in vitiated air enclosure makes a sudden increase of the depression level inside enclosure due to cooling effects. There is a tendency to enhance the fluctuations of the pressure with an increase of ACPH from 3 to 5. With thermal insulation, decreasing the thermal inertia ($\sqrt{\rho C_p \lambda}$) of the envelope by 70% led to a reduction in the depression peak by about 35%. During the fully developed fire, oscillations of the pressure become less sensitive to the intermediate levels of thermal insulation with an increase of ACPH to 5 (cf. Fig.3b). On the other hand, the strong oscillation of the pressure has been identified as a potential risk for the dynamic confinement in order to prevent from hazardous gas leaks.

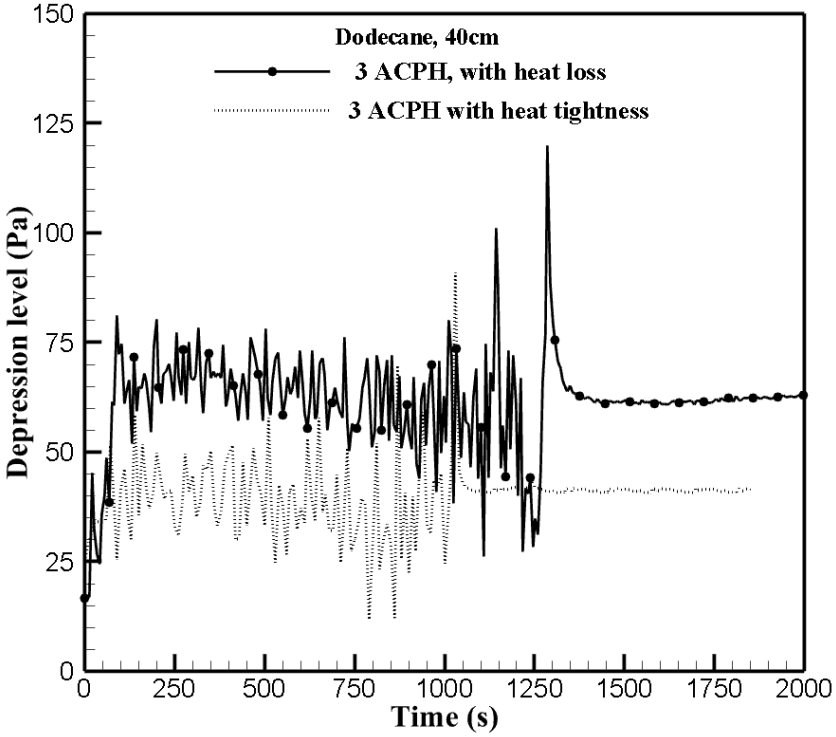

3a) at 3 ACPH

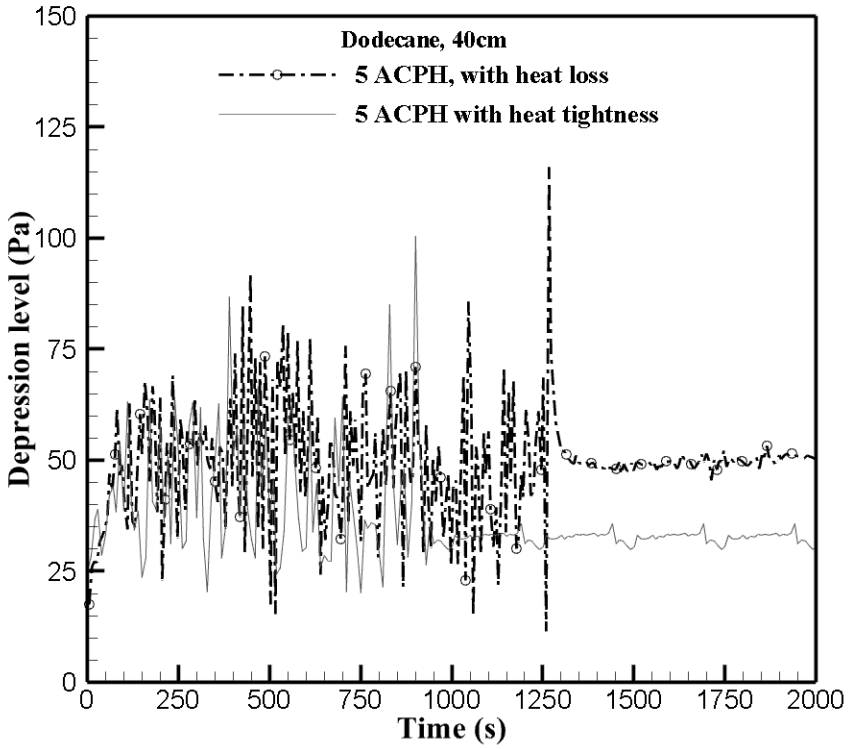

3b) at 5 ACPH

Figure 3. Impact of the intermediate levels of thermal insulation on the pressure inside enclosure

The inlet velocity of fresh air supplied from the admission duct for 3 and 5 ACPH is presented in Fig.4(a, b). After activating the fire, an overpressure inside the compartment causes a reverse flow in the supply admission duct. During the fully developed fire, there is a tendency to enhance the fluctuations of the inlet flow velocity with an increase of ACPH from 3 to 5. At 3 ACPH, the lower depression level with thermal insulation (cf. Fig.3a) around 750 s leads to also a reverse flow in the supply admission duct. Finally, occurrence of flame extinction makes a strong supply of fresh air from the admission duct. With thermal insulation at 5 ACPH, the peak of inlet air velocity at the admission duct is sensitively reduced by a factor of 25%.

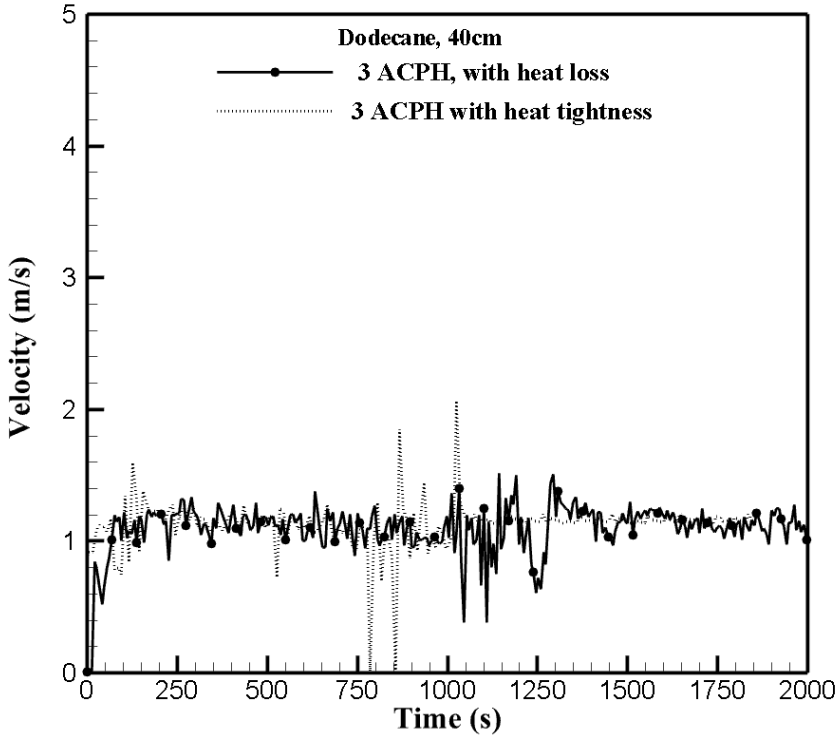

4a) at 3 ACPH

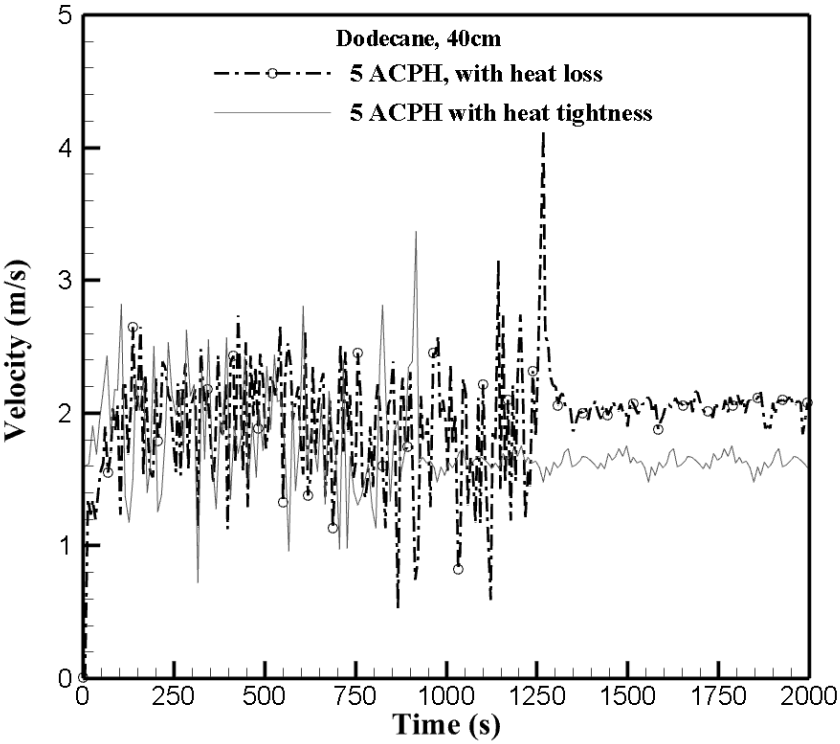

4b) at 5 ACPH

Figure 4. Impact of the intermediate levels of thermal insulation on the inlet air velocity at the admission duct

Influence of the intermediate levels of thermal insulation of enclosure on the mass loss rate at 3 and 5 ACPH is illustrated in Fig.5. With heat loss, a rise of ACPH from 3 to 5 contributes to an increase of the liquid vaporization rate due to enhanced convective mass transfer over the liquid surface. As an illustration (TL4, cf. Fig.1c), the temperature profiles along the height at

different instants are shown in Figure 6(a, b, c). It can be seen that with thermal insulation of enclosure, the hot smoke layer (T>200°C) descends rapidly to the level of liquid surface. As the upper smoke layer is established at 900 s, the hot gas temperature with heat tightness is about 2.5 times of that with heat loss. This results in a significant increase of the mass loss rate due to the enhanced radiative heat feedback from a hot gas layer. When the radiative heat transfer becomes dominant over the liquid surface, the liquid vaporization rate is practically insensitive to an increase of ACPH. In the initial growth phase, burning is fuel-controlled with a stable flame. This is followed by a fully developed, post-flashover phase with oscillations of the mass loss rate due to appearance of an unstable flame in a vitiated air enclosure [5, 15].

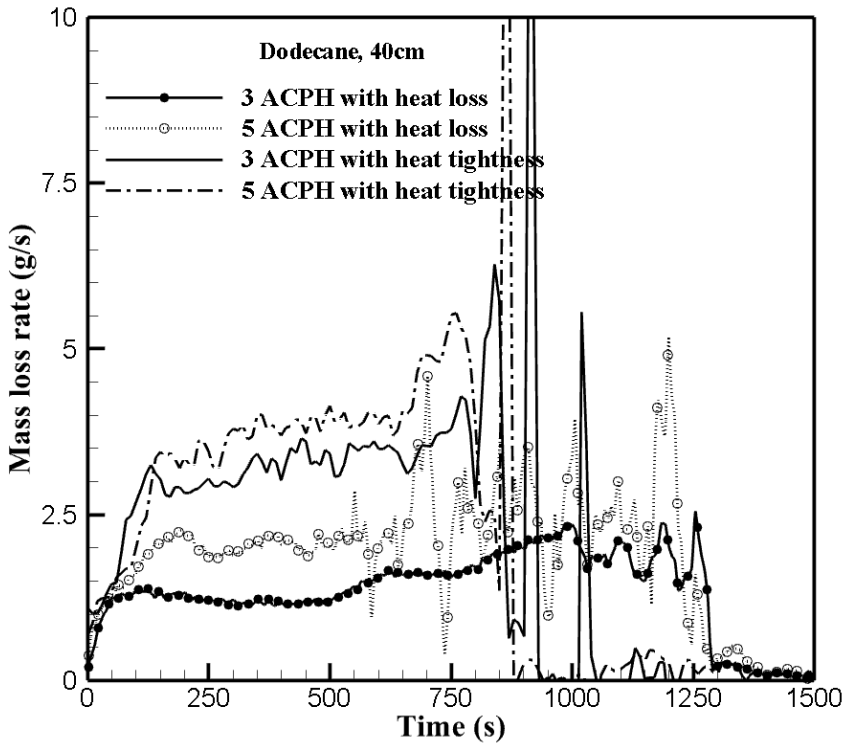

Figure 5. Impact of the intermediate levels of thermal insulation on the mass loss rate for different ACPH

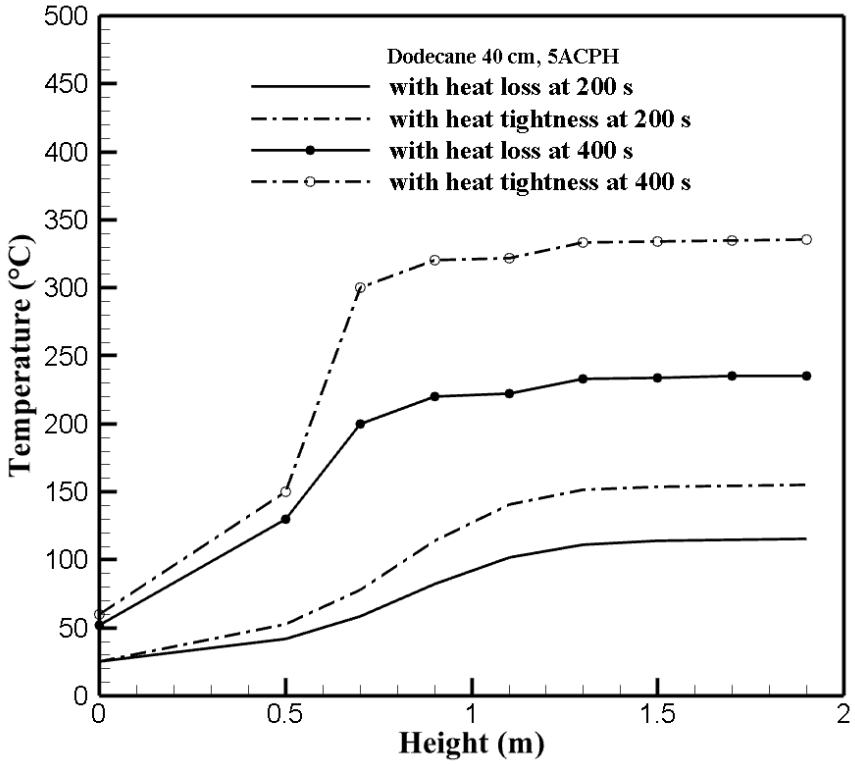

6a) at instants 200 and 400 s

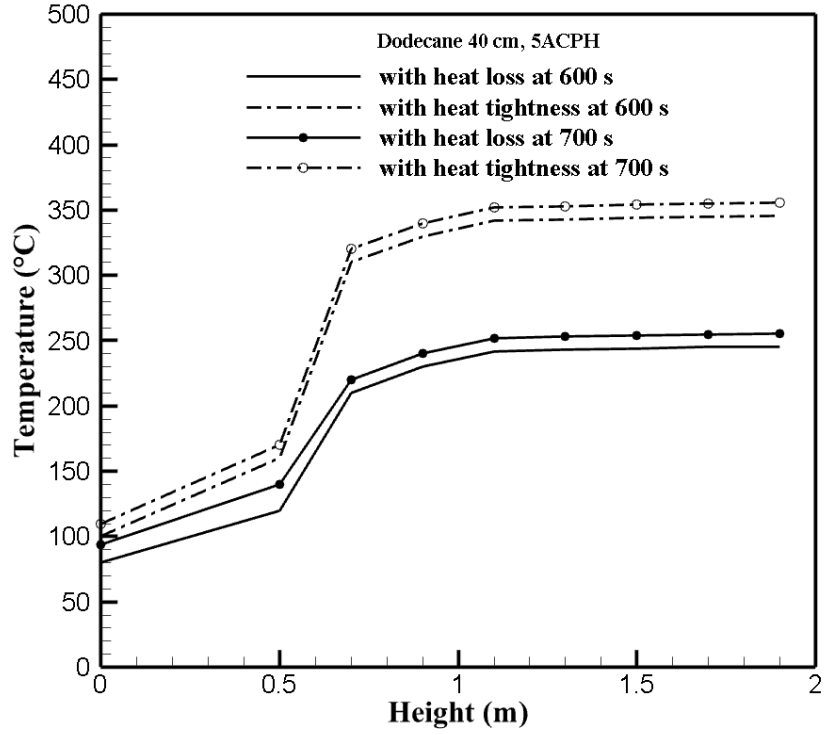

6b) at instants 600 and 700 s

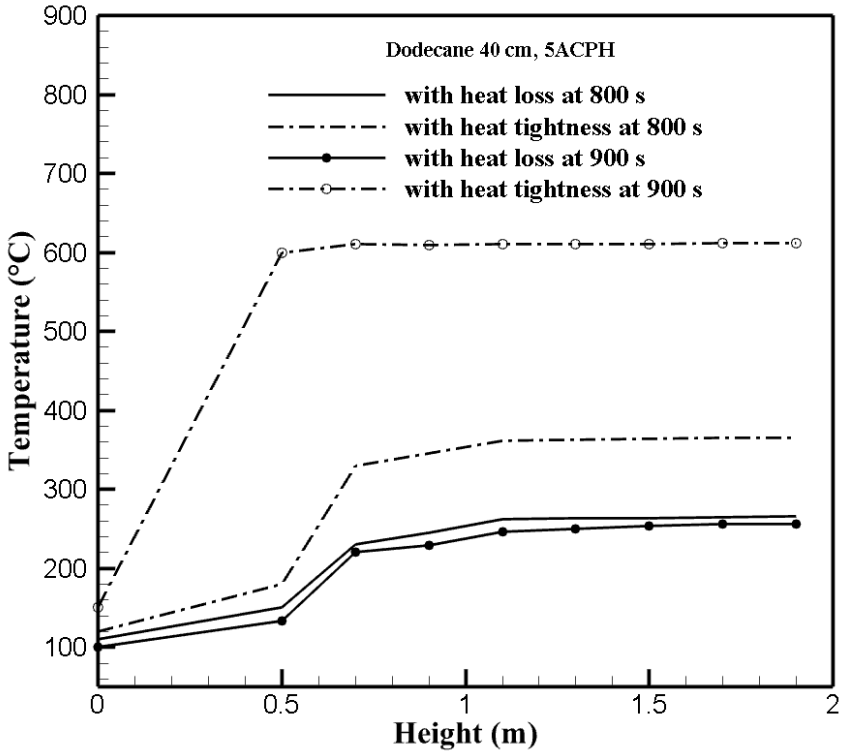

6c) at instants 800 and 900 s

Figure 6. Impact of the intermediate levels of thermal insulation on the temperature profiles along the height at 5 ACPH

A typical evolution of the resulting heat release rate (HRR) at 3 and 5 ACPH is shown in Fig.7(a, b). Note that we lack the ability to accurately quantify the HRR by using oxygen calorimetry in such confined facility. The theoretical HRR is derived from the measured mass loss rate $\dot{m}_F$, as :

$$\dot{Q} = \dot{m}_F \Delta H_c \qquad (2)$$

Here, ΔH_c denotes the energy released per kilogram of fuel consumed (44316 kJ/kg for dodecane). The effective HRR is calculated from the measured oxygen consumption rate at entrance of the extraction duct, as follows :

$$\dot{Q} = \dot{m}_A (Y_{O2,\infty} - Y_{O2}) \Delta H_O \qquad (3)$$

Here, $\dot{m}_A$ denotes the inlet air flow rate (kg/s), Y_{O2} the oxygen mass fraction and ΔH_o the energy released per kilogram of oxygen consumed (13100 kJ/kg).

Note that the boiling point of dodecane is about 220°C, and ignition of such liquid fuel needs a preheating process by using a torch. During preheating phase, heat flowing into the liquid interior over a pool size of 40 cm is uncontrollable. The difference in the early fire growth for the four fire scenarios is observed. By assuming a quadratic growth for the four fire scenarios, an empirical formula is adopted [27] as follows:

$$\dot{Q} = a\, t^2 \qquad (4)$$

The early fire growth factor, a, is defined as 10^3 kW/t_1^2. With heat loss, the growth time, t_1, is about 160 s for 3 ACPH and 632 s for 5 ACPH, corresponding to a fast and slow fire growth, respectively. With thermal insulation, the growth time, t_1, is about 320 s corresponding to a medium fire growth in spite of ACPH. The oscillatory phenomena of the HRR are attributed to the coupling process between the fuel evaporation rate (cf. Fig.5) and the inlet air flow rate (cf. Fig.4), both attached to the intermediate levels of thermal insulation of enclosure. With heat

loss of enclosure (cf. Fig.7a), the HRR curves show a gradual growing trend with a moderate peak of about 90 kW. The oxygen concentration initially present in the enclosure and the one supplied by mechanical ventilation entrain a sufficiently ventilated fire with an almost complete reaction. The effective HRR corresponds approximately to the theoretical one derived from the mass loss rate. It is observed that thermal insulation of enclosure leads to an ultra-fast fire growth (cf. Fig.7b), thus reducing the delay leading to flashover which is clearly identified by a rapid increase of HRR from 40 to 140 kW. The ultra-fast growing fire in a very consistent manner becomes progressively oxygen limited, that is to say ventilation-controlled, and the theoretical HRR is higher than the effective one. The extinction due to unstable combustion in a vitiated air enclosure happened earlier when the wall envelope is more heat-tight.

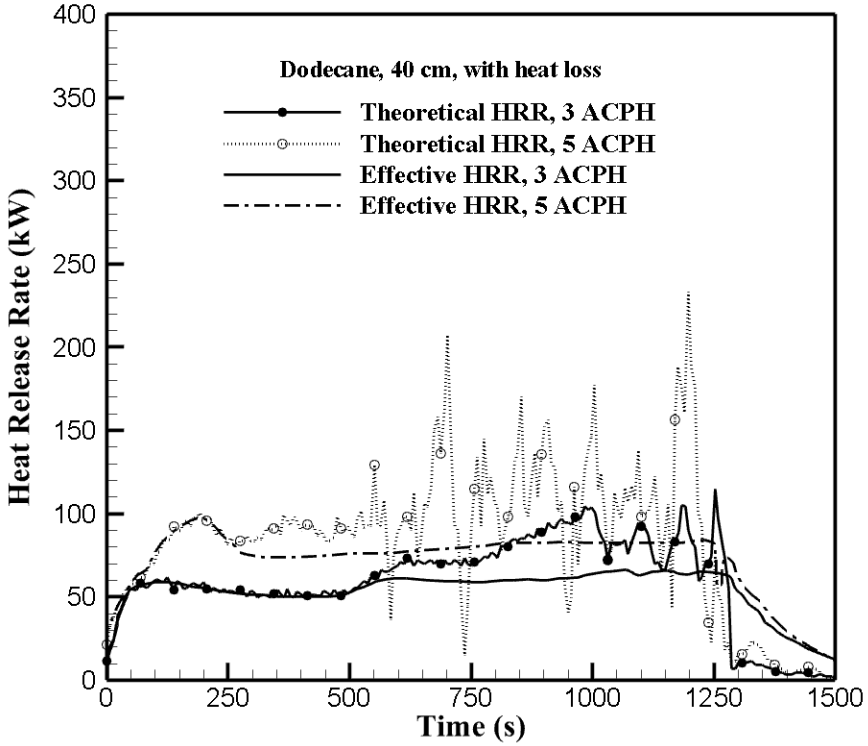

7a) with heat loss

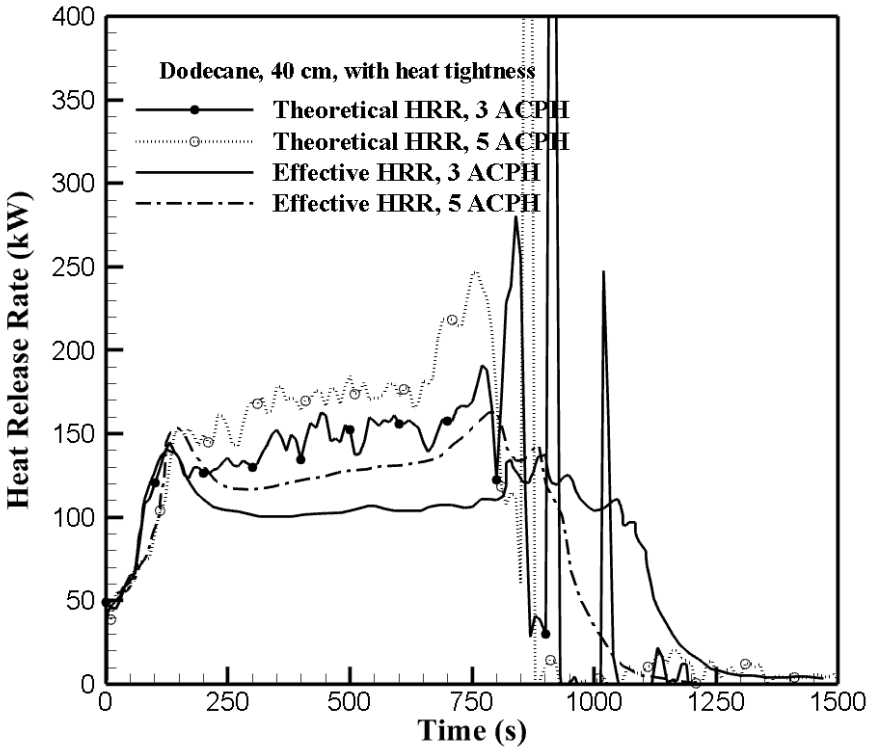

7b) with thermal insulation

Figure 7. Impact of the intermediate levels of thermal insulation on the heat release rate for different ACPH

As an illustration at 5 ACPH, the histories of oxygen concentration at entrance of the extraction duct and near the floor in the vicinity of fire source are shown in Fig.8(a, b). It seems that during the initial growth phase, the oxygen concentration allows to entrain a sufficiently ventilated fire. For most fuels of interest for fire applications, the work of Huggett [28] indicates that combustion occurs when the local oxygen concentration is above a critical value, $Y_{O2,lim,}$ evaluated from this expression :

$$Y_{O2,\,lim} = \frac{C_p\left(T_f - T_m\right)}{\Delta H_o} \qquad (5)$$

The combustion products have an average specific heat C_p of 1.2 kJ/(kg.K), and the adiabatic flame temperature, T_f, is about 1600 K [29]. In a vitiated air enclosure at a temperature of approximately T_m=1000 K (cf. Fig.17), the limiting oxygen mass fraction would evaluate to $Y_{O2,lim}$=0.05. This value is consistent with the visual identification of a visible flame extinction during each fire tests. The fire weakens earlier with thermal insulation and finally stops due to insufficient amount of oxygen even at 5 ACPH. After the fire extinction of the liquid fuel pan, the remaining flames as ghosting flame near the ceiling were not observed. Starting from 700 s, thermal insulation contributes to excessive combustion products, resulting in a decrease of oxygen concentration to about 2% in a fuel-rich hot upper layer near the extraction duct. Thermal insulation of enclosure induces a reduction in oxygen concentration by a factor of 60%. Occurrence of flame extinction makes a sudden increase of oxygen molar fraction to 7% at 900 s with heat tightness and 10% at 1250 s with heat loss due to a return of fresh air from dilution duct. This is followed later by a rise of the O_2 concentration, mainly attributed to air supply thanks to mechanical ventilation. Evolution of the oxygen concentration near the floor (cf. Fig.8b) follows globally the trend near the extraction duct. Thanks to air supply from the admission duct, the oxygen concentration near the floor can be maintained to about 10% at 750 s even with thermal insulation just before occurrence of flame extinction.

A relationship between the oxygen concentration near the floor and the one at entrance of the extraction duct can be established in Fig.9. This relationship presents three parts as a function of the fire regime. For a well-ventilated fire (Y_{O2}>15), the difference in oxygen concentration near the floor and the extraction can be considered negligible. During the underventilated fire phase (5<Y_{O2}<15), a linear relation between the oxygen concentration near the floor and the one at the extraction duct is maintained. During the fire exhaust phase (Y_{O2}<5), an important slope for oxygen concentrations between the floor and the extraction duct is formed.

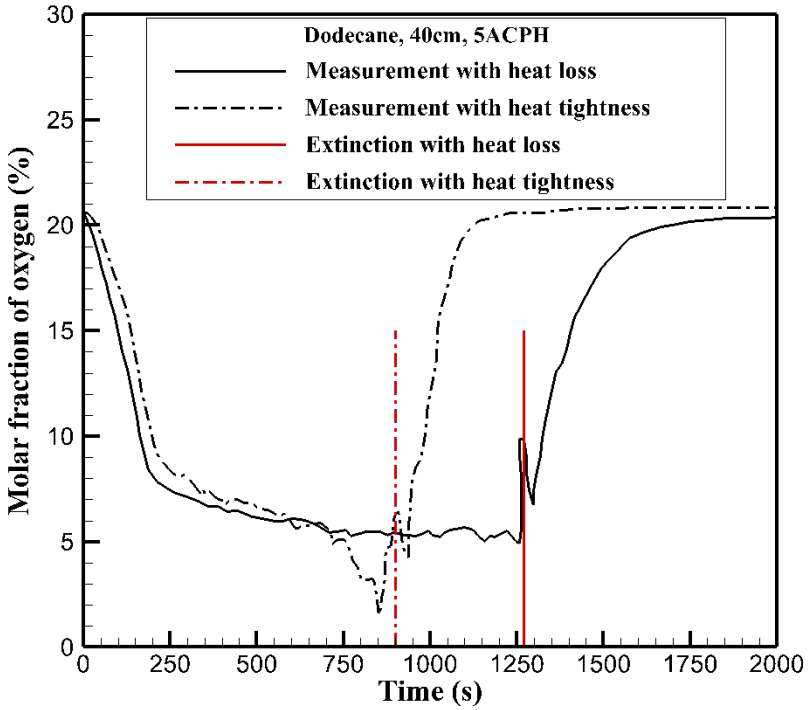

8a) at entrance of the extraction duct for 5 ACPH

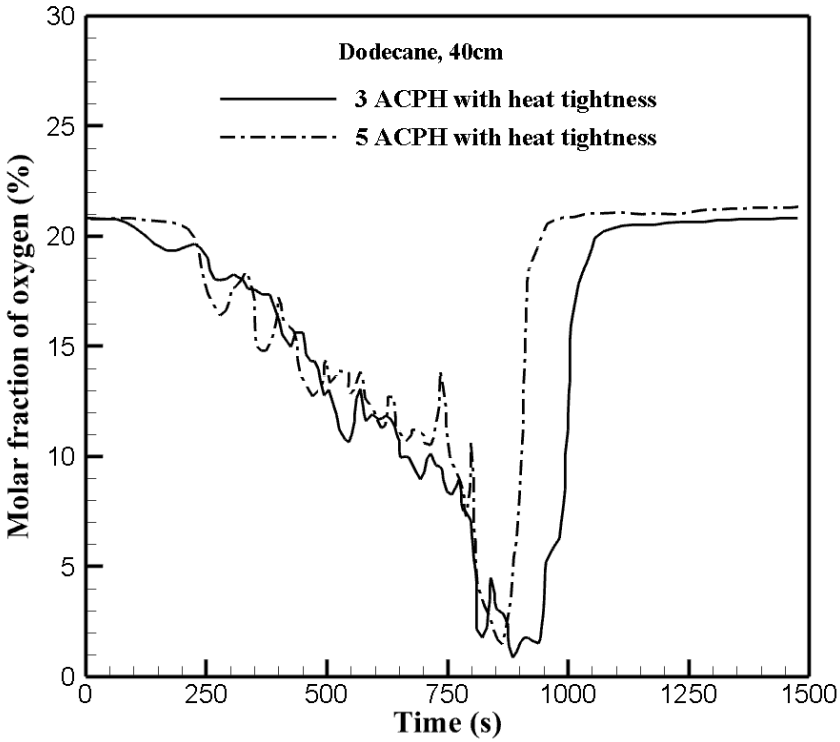

8b) near the floor with thermal insulation for 3 and 5 ACPH
Figure 8. Impact of the intermediate levels of thermal insulation on the history of oxygen concentration

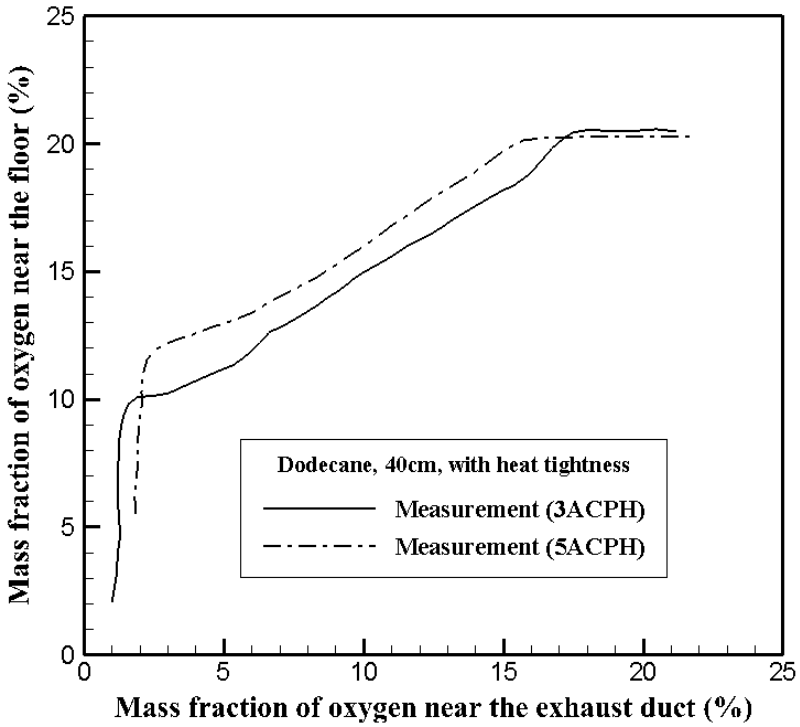

Figure 9. Relationship between the oxygen concentration near the floor and the one at entrance of the extraction duct

Fig.10 shows the history of carbon dioxide concentration at entrance of the extraction duct for 3 ACPH. The CO_2 curve shows a smooth trend during the fully developed fire. When the wall envelope is very heat-tight, oscillations of carbon dioxide concentration are mainly attributed to occurrence of ignition near the extraction duct. Figure 11 shows a linear correlation of CO_2 as a function of oxygen molar fraction, formulated as :

$$[CO_2] = -0.65[O_2] + 0.13 \qquad (6)$$

It seems that a molar fraction of oxygen above 10% is required to stabilize the fire behaviour with a linear increase of CO_2. At the stage where the fire becomes oxygen limited, the CO_2 growth rate decreases due to reduction in the chemical reactivity. Making the compartment more heat-tight does not change the trend of CO_2 formation as a function of O_2.

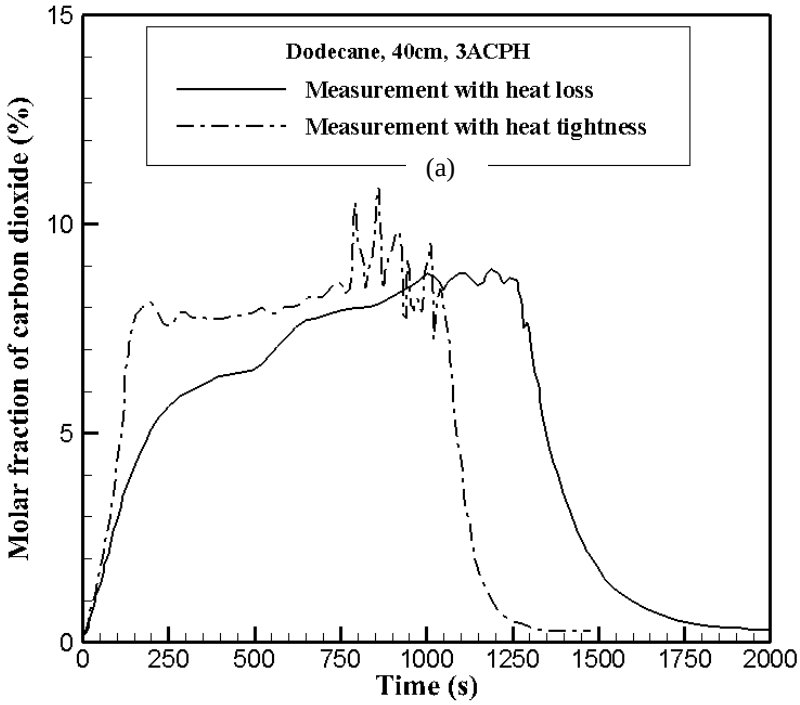

Figure 10. History of the molar fraction of carbon dioxide at the extraction duct for 3 ACPH

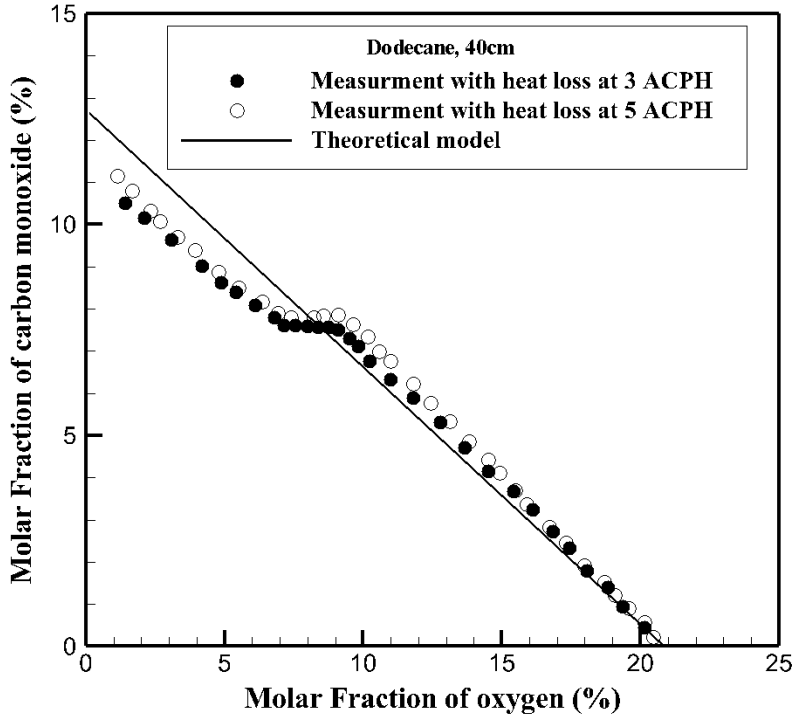

Figure 11. Evolution of carbon dioxide concentration versus oxygen concentration at the extraction duct for 3 and 5 ACPH with heat loss

The empirical correlation for CO production is derived using the theoretical analyses in conjunction with experimental data [30, 31]. This correlation presents three fire regimes as a function of the oxygen concentration, as follows:

$$X_{CO} = \begin{cases} 0 & (X_{O2} \in [X_{MOC},\ X_{O2,\infty}]) \\ -\dfrac{a}{X_{MOC}} \cdot X_{O2} + a & (X_{O2} \in [X_{MOC,co},\ X_{MOC}]) \\ -\dfrac{b}{X_{MOC}} X_{O2} + b + a\left(1 - \dfrac{X_{MOC,co}}{X_{MOC}}\right) & (X_{O2} \in [0, X_{MOC,co}] \end{cases} \quad (7)$$

Here X_{MOC} represents the Minimum Oxygen Concentration for a nearly complete reaction of a fuel-air mixture, and $X_{MOC,co}$ the Minimum Oxygen Concentration for oxidation of CO to CO_2. The CO production is zero when the oxygen concentration is above X_{MOC}, corresponding to a well-ventilated fire. The range of oxygen concentration between $X_{MOC,co}$ and X_{MOC} implies an underventilated fire with a significant CO production due to an incomplete oxidation reaction. The oxygen concentration below $X_{MOC,co}$ results in a maximum CO production, implying a very under-ventilated fire. In Bryner's work [31], oxygen concentration can reach up to zero by using a gas burner to simulate the fire. In the current enclosure fire using a liquid fuel pan, the minimum oxygen concentration is about 2% with thermal insulation (cf. Fig.8).

The previous work [30] proposes also the following relationships as :

$$[CO] = c\sum[C_mH_n] \quad (8)$$

$$[CO] = [H_2] + d\sum[C_mH_n] \quad (9)$$

These correlations (8-9) allow to relate the hydrocarbons and hydrogen concentrations with the CO one. The empirical constants a, b, c and d are given in Table 1. It is found that such constants depend on the range ($0.7 < \phi < 2$ and $2 \le \phi < 3$) of the Global Equivalent Ratio (GER), defined as, $\phi = s \cdot \dot{m}_F / \dot{m}_A$, where s denotes the stoichiometric coefficient. The fuel supply rate $\dot{m}_F$, and air inflow rate $\dot{m}_A$ are controlled by the intermediate levels of thermal insulation via heat transfer and depression level in enclosure. The yields of CO and unburnt hydrocarbons, defined as the fraction of the fuel mass that is converted into these species, are commonly used as an indication for the level of underventilation in the enclosure [32]. To the best knowledge of the authors, only the yields of CO and unburnt hydrocarbons are a function of the GER in well established upper layer of an enclosure fire [32]. In the current enclosure fire, there is unlikely to be sufficient time for two-layer establishment due to the strong fluctuations of HRR (cf. Fig.7). Moreover, identification of the ignition time delay controlled by the fire scenario depends on the time evolution of the local concentration of CO, H_2 and unburnt hydrocarbons near the extraction duct.

As illustrated in Fig.12(a,b), the empirically based correlation (7) for CO production is evaluated as a function of oxygen concentration at entrance of the extraction duct. Both the measurement and correlation indicate that thermal insulation enhances the CO production due to large vaporized fuel. As shown in Fig.13(a,b), the histories of carbon monoxide derived from correlation in transient mode are in a good agreement with the measured one within an error of 6% at 3 ACPH. However, a deviation of more than 40% from the measured CO concentration is found at 5 ACPH with heat loss. This is probably attributed to an increase of the depression level under heat loss conditions, which enhances smoke oscillations (turbulence effect) via

leakage. Figs.14 and 15(a,b) shows the histories of the chemical species such as hydrocarbons and hydrogen concentrations from the measurement and correlations (8-9) at entrance of the extraction duct. The first period, corresponding to sufficiently ventilated conditions $(0 < \phi < 0.7)$ [25] with low CO, H_2 and C_mH_n productions, lasts till 500 s with heat loss, and only 100 s with heat tightness of enclosure. During the second period, we observe a gradual rise of unburnt fuel production with heat loss, and a rapid growth with heat-tightness. During the last period, corresponding to very under-ventilated conditions $(\phi \geq 1.2)$ [25], thermal insulation contributes to the most severe production of unburnt fuels, even for 5 ACPH. The growth rate of the unburnt volatiles becomes faster when the enclosure envelope is very heat-tight, particularly during the post-flashover stage due to lack of oxygen. Globally, the attempt to use an empirical methodology has been successful for the calculation of the unburnt fuels production from the measured oxygen concentration. The empirical correlations are predictive, and applicable for other fire scenarios [30], allowing to assess qualitatively the ignition risk of a fuel rich mixture near the extraction duct if a good similitude is preserved.

Table 1. Empirical constants used in the correlations for CO, C_mH_n and H_2 concentrations

Parameter	With heat loss $(0.7 < \phi < 2)$	With heat tightness $(2 \leq \phi < 3)$
X_{CMO}	11.1%	11.1%
$X_{CMO,\,co}$	6.25%	6.25%
a	1.98	7.45
b	8	1.86
c	1.33	1.2
d	0.75	0.6

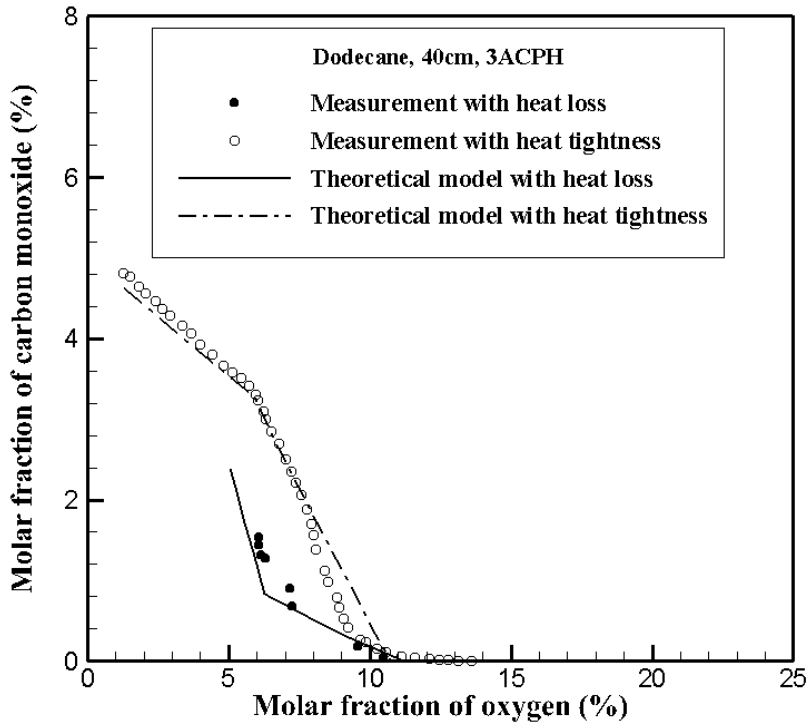

12a) with 3 ACPH

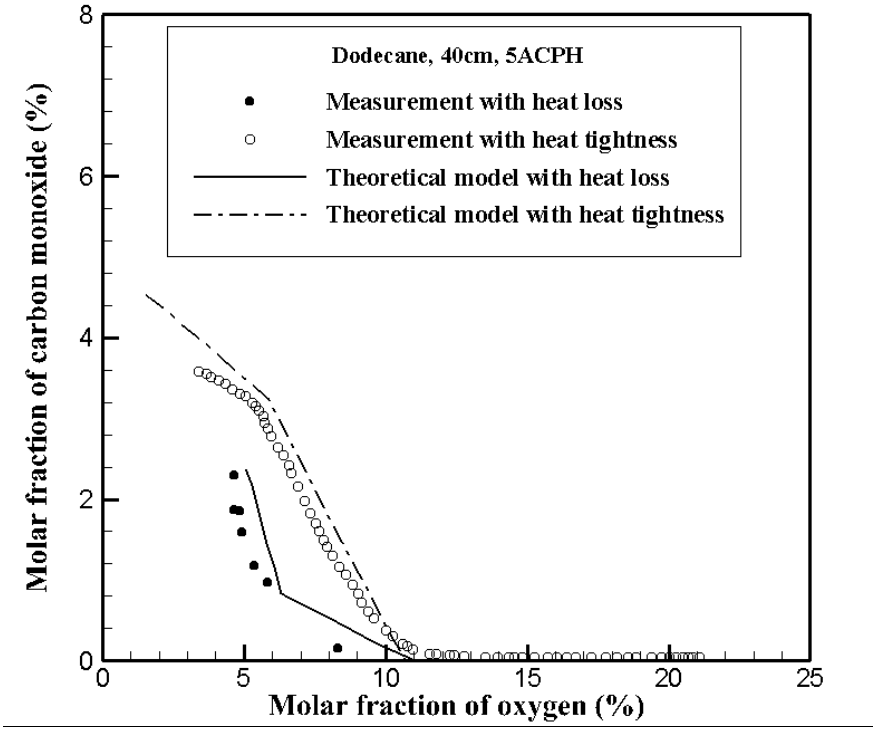

12b) with 5 ACPH

Figure 12. Evolution of carbon monoxide from measurement and correlation as a function of oxygen concentration

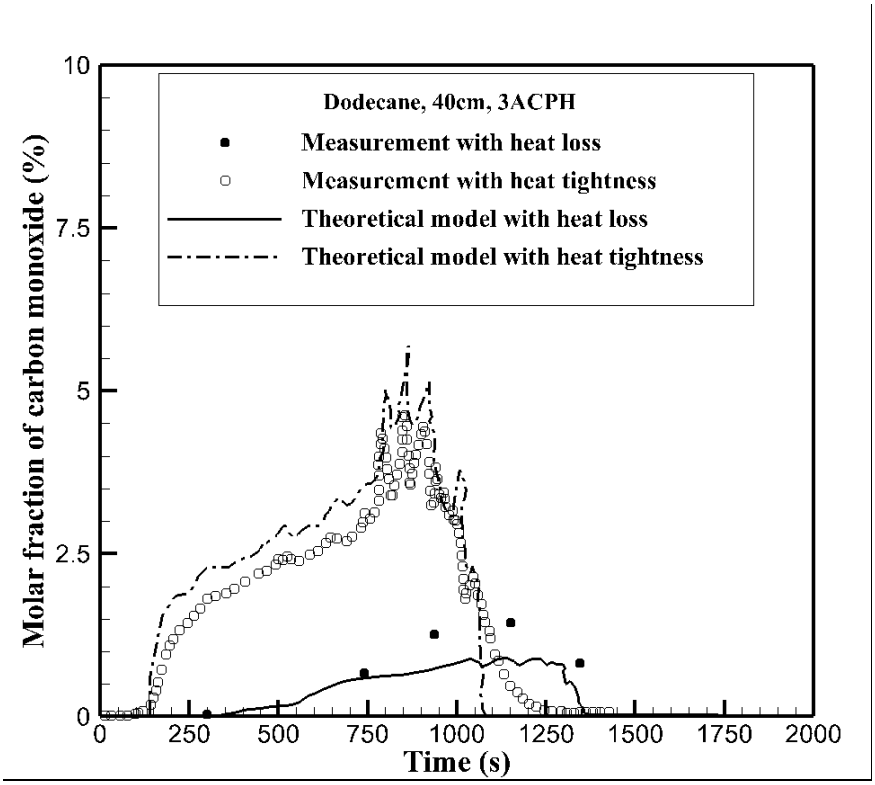

13a) with 3 ACPH

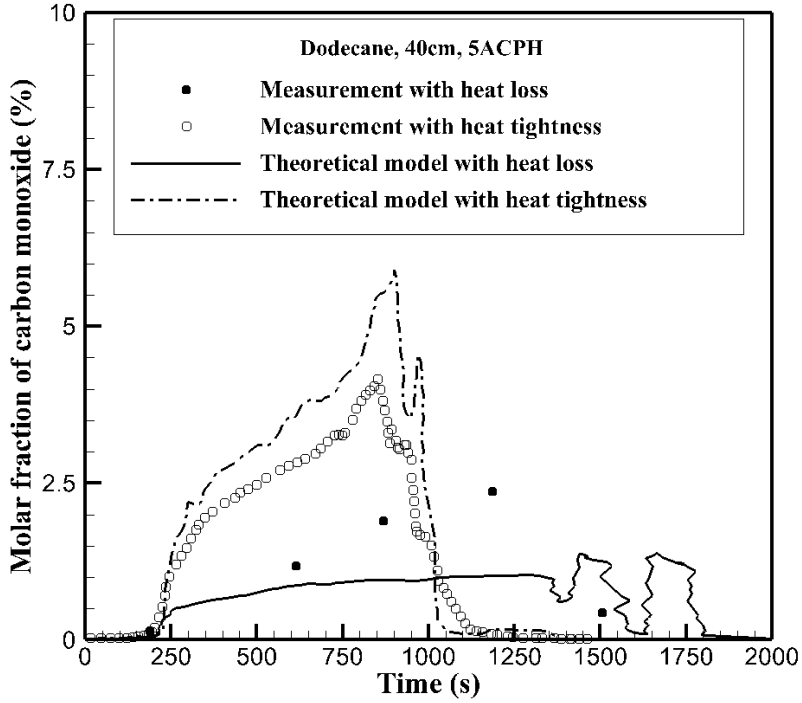

13b) with 5 ACPH

Figure 13. Effect of the intermediate levels of thermal insulation on carbon monoxide concentration in transient mode at entrance of the extraction duct

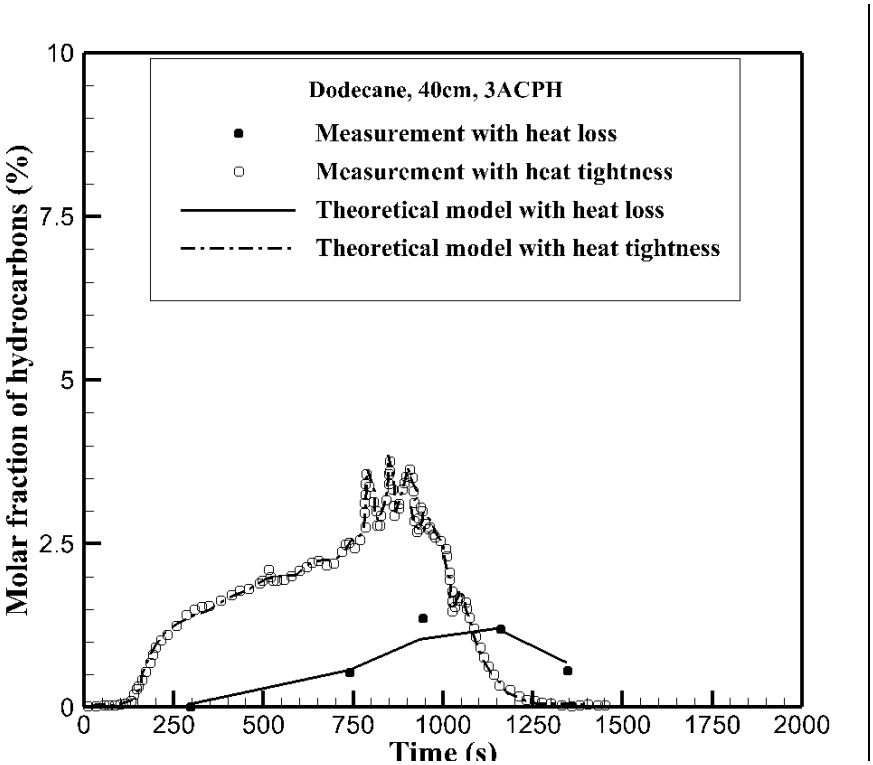

14a) for 3 ACPH

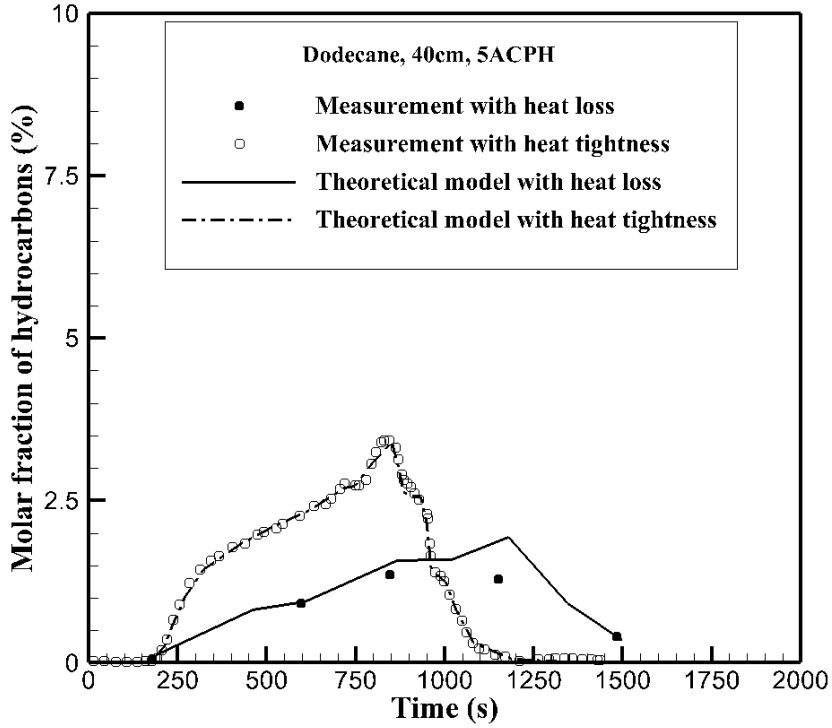

14b) for 5 ACPH

Figure 14. Effect of the intermediate levels of thermal insulation on hydrocarbons concentration in transient mode at entrance of the extraction duct

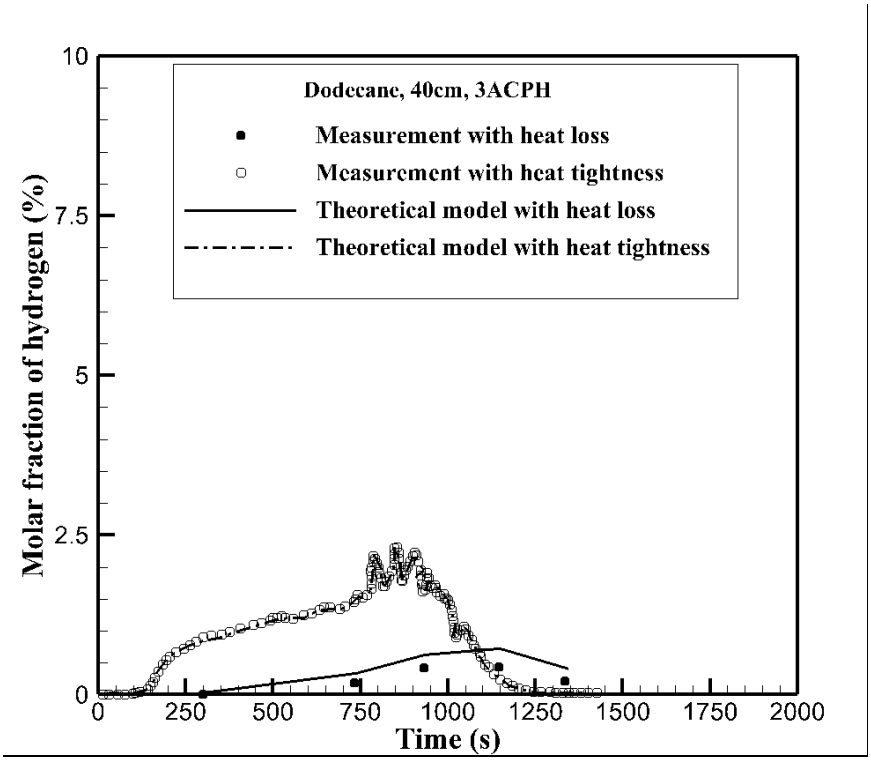

15a) for 3 ACPH

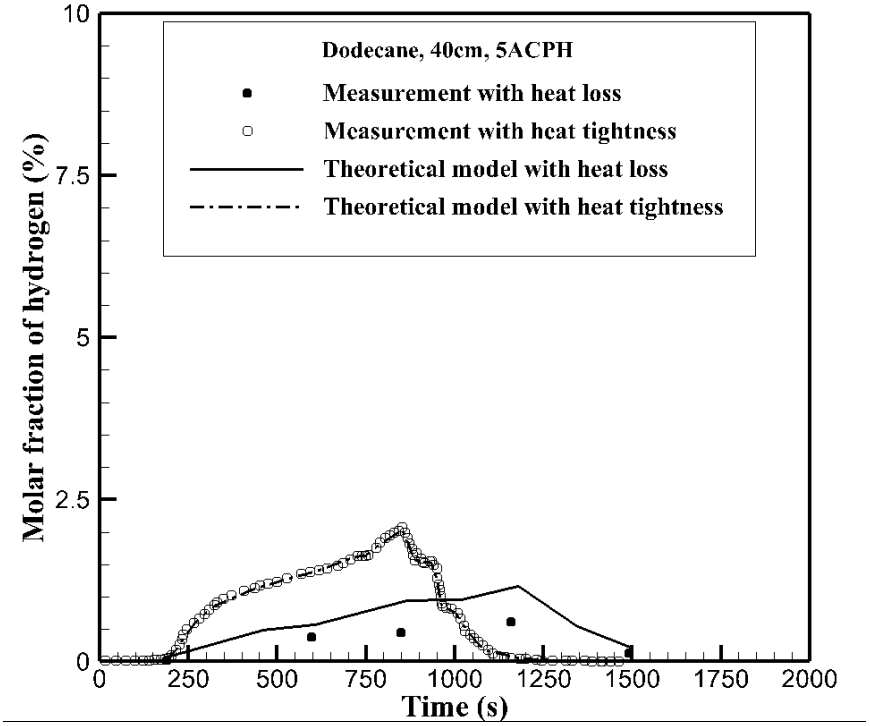

15b) for 5 ACPH

Figure 15. Effect of the intermediate levels of thermal insulation on hydrogen concentration in transient mode at entrance of the extraction duct

In the current enclosure, fire extinction of the liquid fuel pan occurs due to vitiated air with an oxygen concentration below 5% (cf. Fig.8). This section aims to verify theoretically and experimentally Babrauskas's extinction/ignition criteria [33], derived primarily from the Calorimeter apparatus. Theoretically, an auto-inflammation risk takes place when the unburnt fuel concentration is above the Low Flammability Limit (LFL) at the point of Auto-Ignition Temperature (AIT) [33]. The LFL_i of each fuel and the LFL of gas mixtures as a function of both the fuel molar fraction X_i and the gas temperature are determined as follows :

$$LFL_i(T) = LFL_i(T_0)\left[1 - \frac{T - T_0}{1300 - T_0}\right] \quad \text{and} \quad LFL(T) = 100 \times \left[\sum_i \frac{X_i}{LFL_i(T)}\right]^{-1} \tag{10}$$

The Upper Flammability Limit (UFL) can be also calculated as :

$$UFL_i(T) = UFL_i(T_0)\left[1 + \frac{T - T_0}{1412 - T_0}\right] \quad \text{and} \quad UFL(T) = 100 \times \left[\sum_i \frac{X_i}{UFL_i(T)}\right]^{-1} \tag{11}$$

The values of the LFL_i and UFL_i at T_0=25°C as well as AIT for three fuel species [33] are summarized in Table 2.

Table 2. Values of the AIT and LFL/UFL at T_0=25°C for three fuel species

Parameter	CO	H_2	Dodecane
LFL (T_0=25°C)	12.5%	4%	0.6%
UFL (T_0=25°C)	74%	75%	4.7%
AIT (°C)	588	520	204

Note that even at a more developed stage with an enhanced evaporation rate, the concentration of the unburnt volatiles is never above the Upper Flammability Limit (UFL) with a value of about 20%. The molar fraction of unburnt volatiles in addition to the LFL of the gas mixtures near the extraction duct is presented in Figure 16(a-d). According to the visual identification, occurrence of auto-ignition inside the extraction duct was observed experimentally at 3 or 5 ACPH with heat tightness (cf. Figs.16b, d) and only at 5 ACPH with heat loss (cf. Fig.16c). An auto-ignition of a fuel rich mixture with presence of combustion products near the extraction duct represents very complex chemistry and physical processes, there is still a lack of knowledge for complete understanding of such random phenomenon. In regards to ignition risk in a connected exhaust system, the three characteristic stages can be described, as follows :

i) In the early stages of a fire, starting from 350 s with heat loss and 200 s with thermal insulation, a stratified hotter unburnt fuels layer with a concentration above the Lower Flammability Limit (LFL) is formed near the ceiling. It seems that the point of Auto-Ignition Temperature of about 220°C for the primary fuel as dodecane (cf. Tab.2) is not high enough for triggering an auto-ignition of a fuel rich mixture in addition to combustion products. It is noticeable that the auto-ignition temperature of a mixture is chemical composition-dependent (hydrocarbons, CO, H_2, etc.), and difficult to be accurately quantified through bench-scale experiments.

ii) With a long time delay in a range of 16 to 21 min in the current study, the energy released per mass of oxygen consumed allows the smoke temperature to raise above 350°C, high enough for an auto-ignition of a mixture of the unburnt gases and vitiated air. However, during this stage, the large vaporized fuel due to enhanced heat transfer does not completely contribute to the heat release. Thus, a part of the fuel vapor accumulates with a concentration considerably higher than LFL, particularly with thermal insulation. Consequently, there is insufficient oxygen available near the extraction duct for triggering the ignition.

iii) Occurrence of flame extinction with an oxygen concentration below 5% makes a sudden increase of the depression level inside enclosure due to cooling effects. This induces a sudden supply of fresh air from dilution duct, characterized by a sharp increase of oxygen concentration to 10% (cf. Fig.8a) at the extinction point of about 1250 s with heat loss and to 7% at 900 s with heat tightness. The supply of fresh air leads to a rapid dilution of unburnt fuel with a concentration close to a stoichiometric fuel-air mixture. This is ideal for triggering the ignition of a fuel rich mixture with a peak reaching a typical flame temperature higher than 550°C. With heat loss of enclosure (cf. Fig.16c), occurrence of auto-ignition near the extraction duct was consistently observed at 5 ACPH with a longer time delay of about 1320 s after the extinction at 1250 s. Thermal insulation of enclosure (cf. Fig.16d) contributes to a significant reduction in the ignition delay time to about 780 s due to fast-growing fires.

It is found that the delay for the transition from extinction of the fuel pan to ignition near the extraction duct is about 60-70 s. With heat loss of the enclosure at 3 ACPH (cf. Fig.16a), after extinction at 1300 s, dilution of the unburnt fuel from the return of fresh air makes its concentration decrease below LFL during the transition delay. The temperature peak was not experimentally detected by the thermocouple near the extraction duct. This implies that an auto-ignition of the unburnt gases does not take place there, probably attributed to cooling of the smoke. Note that the response time of the thermocouples used in the experiment is close to a second by including thermal mass inertia and accumulation of soot particles. Besides, raw thermocouple data are corrected by heat transfer effects via convection and radiation. During auto-ignition of the unburnt gases, accurate measurement of flame temperature by using

thermocouples is difficult by taking into account a multitude of potential errors, including surface reactions, radiation, convective gain or loss. The leakage of the experimental facility is also uncontrollable during each fire tests.

Globally, the compartment fire dynamics depend on the Global Equivalence Ratio (GER) associated with pool size, ACPH and fuel type. In a specific configuration with an admission duct placed closer to the floor and an exhaust near the ceiling, the GER above 1.5 represents a set of dangerous conditions for spontaneous ignition at entrance of the extraction duct (cf. Figs.16a-d). The auto-ignition of unburnt fuels at the extraction duct occurs without needing a pilot flame as ghosting flame. To the knowledge of the authors, any attempt to draw a general conclusion for all configurations is discouraged. In order to obtain a good similitude between various scale compartments, a preservation of the ratio between heat release rate and characteristic length with a constant Froude number is needed.

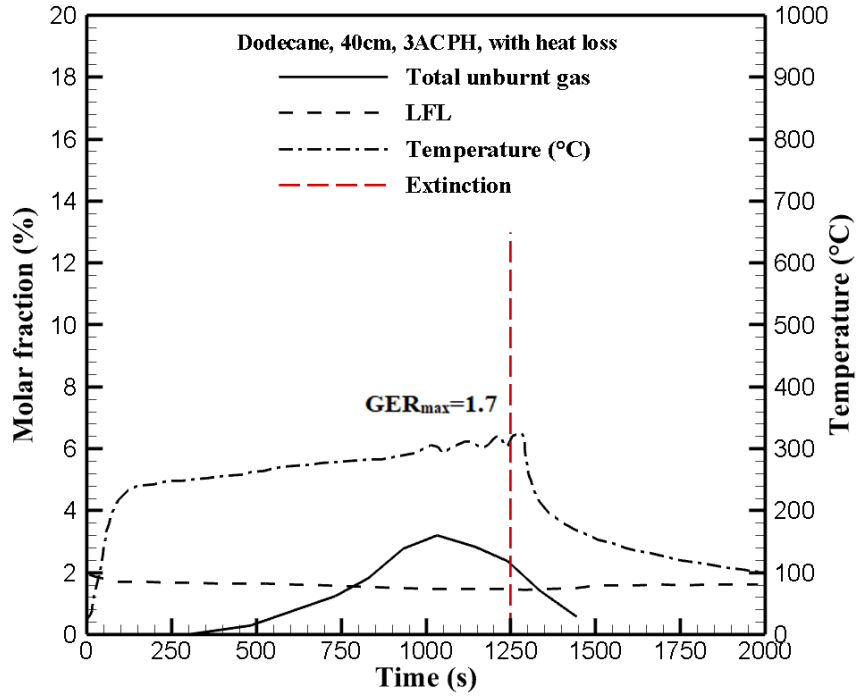

16a) with heat loss at 3 ACPH

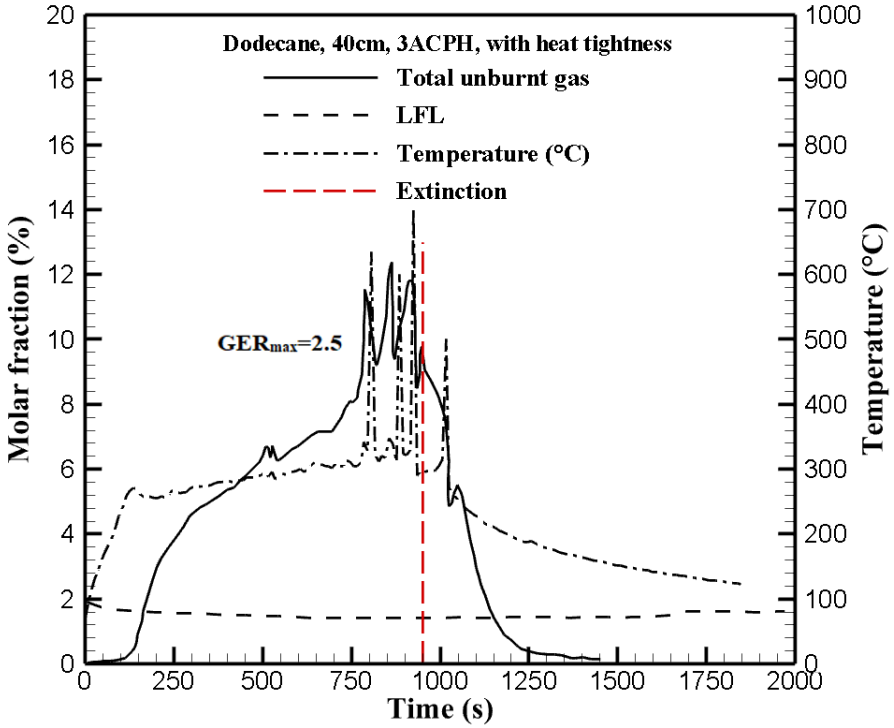

16b) with heat tightness at 3 ACPH

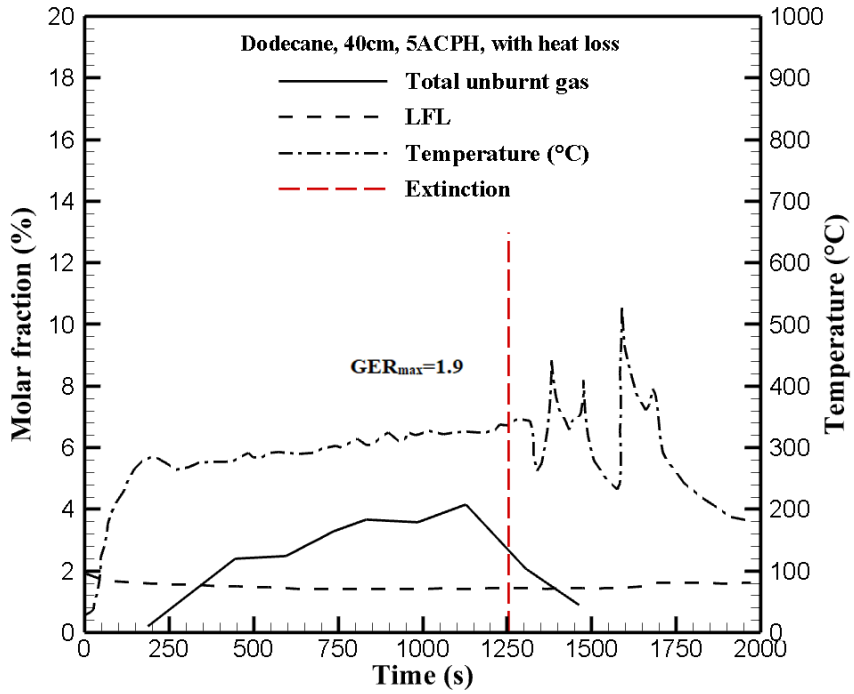

16c) with heat loss at 5 ACPH

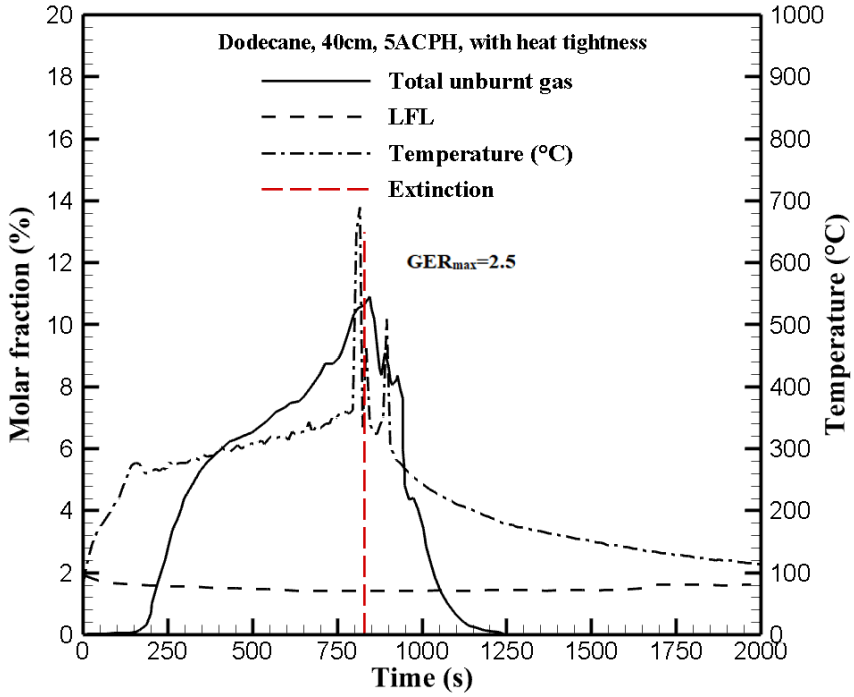

16d) with heat tightness at 5 ACPH

Figure 16. Risk assessment of unburnt gas ignition at entrance of the extraction duct

Fig.17(a,b) shows the histories of gas-phase temperature at a thermocouple tree in the center of the compartment at a height of 60 cm (TL5, cf. Fig.1b, c) from the liquid surface. It is seen that thermal insulation of the wall envelope at 3 ACPH causes a strong decreasing trend of the temperature from 120 s. This is attributed to the flame moving from the fuel source due to lack of oxygen, expanding radially and horizontally towards the air inlet [6]. An inverse dependence of the gas temperature with time is observed. This is contrary to the trend at the extraction duct where the gas temperature rises with time due to energy accumulation. The auto-ignition near the extraction duct at 900 s (cf. Fig.17a) makes an oscillation of the smoke layer temperature,

and its impact on the gas temperature in the vicinity of fuel pan is characterized by a sharp temperature spike. An increase of ACPH to 5 (cf. Fig.17b) helps maintain a relatively high temperature level for many minutes only with a slightly decreasing trend. As shown in Fig.6c, thickness of the hot smoke layer (T>200°C) increases from 1.3 m with heat loss to 1.9 m with thermal insulation. Thus, impact of the temperature oscillation within the smoke layer due to ignition near the extraction duct on the centerline gas temperature seems less remarkable with heat loss. Finally, a sharp decreasing trend of the gas temperature from 20 min with heat loss and 16 min with heat tightness corresponds to the onset of extinction.

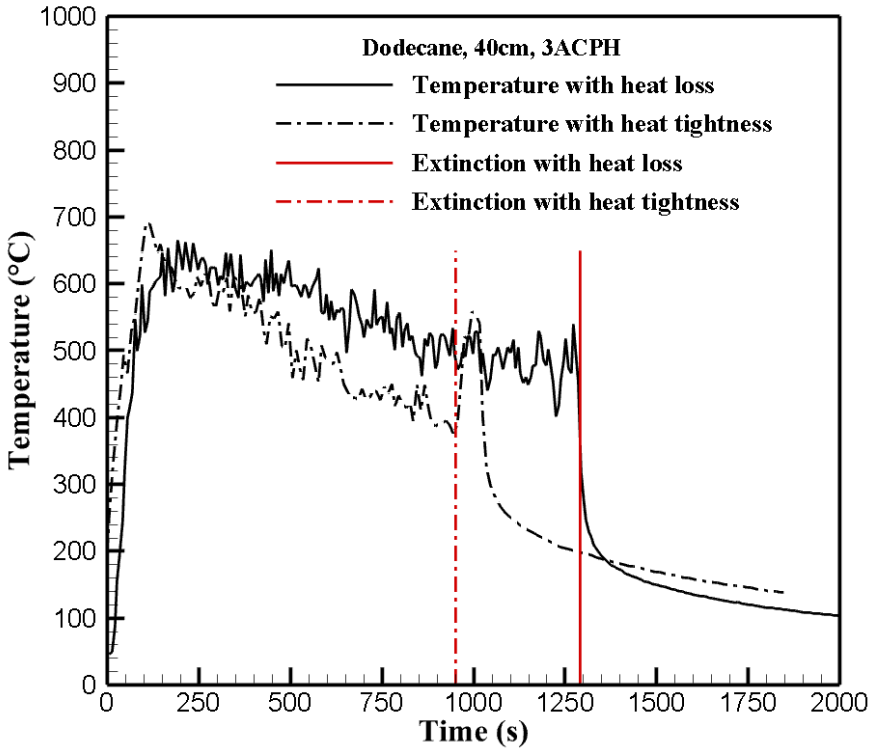

17a) at 3 ACPH

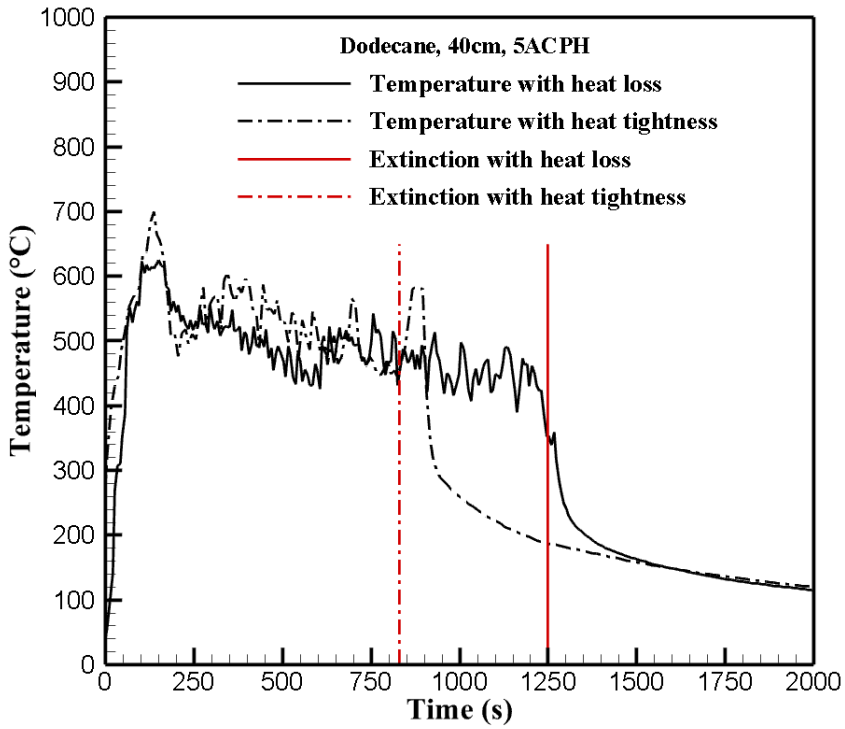

17b) at 5 ACPH

Figure 17. Influence of heat permeability on the history of gas-phase temperature in the center of the compartment above the liquid pool fire

CONCLUSION

In summary, heat-tightness of enclosure can sensitively increase the liquid vaporization rate, and reduce the air supply flow rate due to a decrease of depression level inside enclosure. This implies that burning is quickly ventilation controlled with thermal insulation of enclosure, forming significant amount of unburnt volatiles. If the concentration of unburnt volatiles is higher than LFL, and the fire has been established for sufficiently long (in this case, more than 15 min), there is significant risk of ignition inside the extraction duct without needing a pilot flame like a ghosting one. Occurrence of an ignition of the hotter unburnt fuels at entrance of the extraction duct is attributed to a return of air from dilution duct at the stage of fire extinction which induces a sudden increase of depression level inside enclosure. An ignition can happen early near the extraction duct, as long as the enclosure remains sufficiently heat tight. Globally, the causes involved for occurrence of auto-ignition near the extraction duct are amount of accumulated unburnt volatiles above LFL, gas temperature above 350°C, oxygen concentration above 7% with heat tightness and 10% with heat loss, and phenomena leading to fire extinction with an oxygen concentration below 5%.

The intermediate levels of thermal insulation of enclosure appears a critical factor for time delay of occurrence of ignition via vaporization rate of condensed fuel and depression level inside enclosure. The work is continuing with the aim of improving the evaluation of auto-ignition temperature near the extraction duct by analyzing a more detailed chemical species. The future investigation aims also to identify the scale effect of enclosure on heat fluxes over the liquid surface via radiation contribution from flame, smoke layer and hot walls.

REFERENCES

[1] Gojkovic D., Initial backdraft experiments, Report 3121, Department of Fire Safety Engineering, Lund University, Sweden, 2000.

[2] A. Horvat and Y. Sinai, Numerical simulation of backdraft phenomena, Fire Saf. J. 42 (2007) 200-209.

[3] Lassus, J., Studer, E., Garo, J.P., Vantelon, J.P., Jourda P. and Aine, P., Influence of ventilation on ignition risk of unburnt gases in the extraction duct of under ventilated compartment fire. Combust. Sci and Tech, 182(2010)517-528, doi.org/10.1016/j.ijthermalsci.2013.07.015.

[4] Prétrel, H., le Saux W. and Audouin L., Pressure variations induced by a pool fire in well-confined and force-ventilated compartment, Fire Safety, 52(2012) 11-24, doi:10.1016/j.firesaf.2012.04.005.

[5] Zavaleta, P. and Audouin, L., Cable tray fire tests in a confined and mechanically ventilated facility, Fire and Materials, 42(2018) 28-43, doi:10.1002/fam.2454.

[6] Wahlqvist, J. and Van Hees, P., Validation of FDS for large-scale well-confined mechanically ventilated fire scenarios with emphasis on predicting ventilation system behavior, Fire Safety, 62(2013) 102-114, doi.org/10.1016/j.firesaf.2013.07.007.

[7] Hu, Z., Utiskul, Y., Quintiere, J.G., Trouvé, A., A comparison between observed and simulated flame structures in poorly ventilated compartment fires, Fire Safety Science – Proceedings of the eighth International Symposium, (2005) 1193-1204,

[8] Takeda, Oscillatory phenomenon and inverse temperature profile appearing in compartment fires, Combustion and Flame, 61(1985) 103-105.

[9] Peatross, M.J. and Beyler, C.L. Ventilation effects on compartment fire characterization. In Fire Safety Science – Proceedings of the Fifth International Symposium, Vol.5, pp.403-414, 1997.

[10] Utiskul, Y. Theoretical and experimental study on full-developed compartment fires, Report 2006, Fire Engineering, University of Maryland, USA, 2006.

[11] Tewarson, A., Lee, J.L. and Pion, R.F. The influence of oxygen concentration on fuel parameters for fire modelling. Symp. (Int.) Combust., 18, 563-570, 1981.

[12] Orloff, L. and de Ris, J. Froude modelling of pool fires. 19th International Symposium on Combustion. The Combustion Institute, pp.885-895, 1982.

[13] Hamins, A., Yang, J.C. and Kashiwagi, T. A global model for predicting the burning rates of liquid pool fires. Technical Report NISTIR-6381, NIST, 1999.

[14] Beaulieu, P., and Dembsey, N. Effect of oxygen on flame heat flux in horizontal and vertical orientations, Fire Safety J., 43, 410-428, 2007.

[15] Vilfayeau, S., Ren, N., Wang Y. and Trouvé A., Numerical simulation of under-ventilated liquid-fueled compartment fires with flame extinction and thermally-driven fuel evaporation. Proceedings of the Combustion Institute, 35(2015) 2563–2571, doi.org/10.1016/j.proci.2014.05.072.

[16] T. Sikanen and S. Hostikka, Predicting the heat release rates of liquid pool fires in mechanically ventilated compartments, Fire Safety J. 91(2017) 266-275.

[17] B. Merci and K. Van Maele, Numerical simulations of full-scale enclosure fires in a small compartment with natural roof ventilation, Fire Safety Journal, (2008) 495-511.

[18] W. Wegrzynski and G. Vigne, Experimental and numerical evaluation of the influence of the soot yield on the visibility in smoke in CFD analysis, Fire Safety Journal, 91(2017) 389-398.

[19] S. Hostikka, R. Kallada, U. Riaz, T. Sikanen, Fire-induced pressure and smoke spreading in mechanically ventilated buildings with air-tight envelopes, Fire Safety Journal, 91 (2017) 380-388.

[20] Cabeza LF, Castell A, Medrano M, Martorell I, Pérez G, Fernandez I, Experimental study on the performance of insulation materials in Mediterranean construction. Energy and Buildings, 42 (2010) 630-6.

[21] C. Forneau, C. Delvosalle, H. Breulet, S. Desmet, S. Brohez, Comparison of fire hazards in passive and conventional houses, Chem. Eng. Trans., 26 (2012) 375-380.
[22] Sinai, Y.L., Comments on the role of leakages in field modelling of under-ventilated compartment fires, Fire Safety Science, 35-1(1999) 11–20, doi.org/10.1016/S0379-7112(99)00005-3.
[23] Nasr, A., Suard, S., El-Rabii, H., Garo, J.P., Gay L. and Rigollet, L., Heat feedback to the fuel surface of a pool fire in an enclosure, Fire Safety, 60(2013) 56–63, doi:10.1016/j.firesaf.2012.12.005.

[24] D. Zigrang and N. Sylvester, A review of explicit friction factor equations, Transactions of the ASME, 107:280-283, 1985.
[25] B. Magnognou, J. P. Garo, B. Coudour and H. Y. Wang, Risk assessment of unburnt gas Ignition in an exhaust system connected to a confined and mechanically ventilated enclosure fire, Journal of Fire Safety, 91:291-302, 2017.
[26] E.E. Zukoski , Fluid dynamics aspects of room fires, First International Symposium on Fire Safety Science, (1984) 1-30.
[27] NFPA (National Fire Protection Association), Standard growth curves, BRE-Project**,** 2009.
[28] C. Huggett, Estimation of the rate of heat release by means of oxygen consumption, Fire and Materials, Vol.12, pp.61-65, 1980.
[29] C. Beyler, Flammability limits of premixed and diffusion flames, SFPE handbook of Fire Protection Engineering (3rd Ed), National Fire Protection Association, Quincy, MA, 2003.
[30] J. Lassus, L. Courty, E. Studer, J.P. Garo, P. Jourda and P. Aine, Estimation of species concentration during a fire in a reduced scale room, Journal of Fire Science, 34(1) (2016) 30-50.
[31] N.P. Bryner, E.L. Johnsson, W.M. Pitts, Carbon monoxide production in compartment fires: reduced-scale enclosure test facility, National Institute of Standards and Technology, NISTIR-5568, 1994.

[32] The SPFE Handbook of Fire Protection Engineering, National Fire Protection Association, Greenbelt, MD, Chapter 16:486-528. DOI 10.1007/978-1-4939-2565-0, 2016.

[33] Babrauskas, V., Ignition Handbook, Fire Science Publishers, Chapter 4:41-140, 2003.